

Molecular-Dynamics Simulation of Vulcanian Eruption

Satoshi YUKAWA* and Nobuyasu ITO†

*Department of Applied Physics, School of Engineering, The University of Tokyo,
7-3-1, Hongo, Bunkyo-ku, 113-8656, JAPAN*

Vulcanian explosive eruption, which is a nonlinear and nonequilibrium abrupt dynamics of magma-gas mixture, is modeled by a two-component Lennard-Jones particle system. Molecular-dynamics simulation of a shock-tube experiment gives consistent results with a explosive eruption picture of volcanology; Shock wave and expansion wave are reproduced. In addition bubble nucleation of a gas component in the magma melt and spinodal-like decomposition are observed in the simulation. The result is also compared with a continuum hydrodynamic model; Qualitative features of continuum dynamics are reproduced by the present model. We find that the particle description of dynamics is an effective method in such kind of abrupt dynamics.

KEYWORDS: Vulcanian eruption, Lennard-Jones particle, molecular dynamics simulation, shock tube

Volcanic eruption is complicated physical phenomena and the physical understanding has not been well established yet; The problem is to understand nonlinear and nonequilibrium dynamics of magma-gas mixture accompanied by phase transitions.¹⁻³ Existence of gas, which is mainly H₂O, is sometimes forgotten, but it is pointed out that such gas component plays an important role in explosive eruption.⁴ Type of volcanic eruption is classified into three classes by chronological behavior; One is so-called Vulcanian type eruption, which is widely observed in Japanese volcanos. This type is characterized by an intermittent explosive eruption and formation of a lava dome. These features are determined by physical properties of magma; Specifically viscosity of magma controls them.

In this paper, we study Vulcanian eruption, because its explosive mechanism will be the most interesting physically, in particular, in the context of nonequilibrium physics; In the volcanology, an eruption picture is considered as follows: A stage of eruption dynamics consists of a magma chamber and a conduit. Top of conduit is covered by a lava dome. In a top of magma chamber or a lower part of conduit, a gas component is almost completely dissolved into the magma melt. In the upper region of saturated magma, the gas is exsolved according to the equilibrium solubility law. As decreasing the lithostatic pressure, volume fraction of gases is increasing. At the beginning of eruption, pressure of the magma-gas mixture is considered to increase, although the mechanism is not clear yet. When the lava dome cannot support this overpressure, it disrupts the lava dome. At the next moment, two shock waves appear and propagate; One is a shock wave formed between atmosphere and compressed air and it propagates upward. Another is decompression wave in magma-gas melt and it goes to opposite direction. During the eruption it is observed that the transition from the laminar flow of bubbly melt to the turbulent flow of gas-magma dispersion in the conduit. This transition layer determines the front of fragmenta-

tion wave which propagates downward. At the moment, viscosity of magma-gas mixture is drastically changed abruptly about the order of $10^{12} \sim 10^{15} \text{Pa} \cdot \text{s}$.

There have been many theoretical investigations of Vulcanian eruption in the volcanism study. In 1995, Woods proposed the model for magma flow in conduit;⁵ In his model magma-gas mixture is treated as a one-dimensional nonviscotic compressible fluid with single component. This model can capture physical properties of dynamics in some sense. But treatment of dynamics is not well satisfied; For example, flow is treated as isentropic one, though bubble nucleation accompanies the eruption. There are some other phenomenological models, but the present understanding of the eruption dynamics is still unsatisfactory in the context of nonequilibrium physics.^{2,3}

Recent progress of experimental techniques enables us to compare such theoretical model with experimental results; These experiments are called as shock-tube experiment.⁶⁻⁹ In the experiment, analogue materials of magma-gas mixture, such as viscoelastic materials and powder, are used. It is observed that the behavior of explosion depends on the viscosity of analogue materials. Thus a non-viscotic treatment in a theoretical study is not sufficient.

In this paper, we try to establish a computational microscopic model of Vulcanian eruption; So to say, we want to make “an Ising model of Vulcanian eruption”. Here we describe dynamics of the mixture by microscopic particle dynamics. A particle dynamics simulation can be regarded as an ideal shock-tube experiment, because we can calculate macroscopic quantities. In addition, using the particle dynamics, we can also reproduce hydrodynamic behavior described by a continuum description of Navier-Stokes equation. Even in Newtonian dynamics, we can produce macroscopic behavior in linear nonequilibrium thermodynamic regime.¹⁰⁻¹³ Moreover we can also discuss phenomena in far from equilibrium state, which are not captured by continuum descriptions based on local equilibrium. Thus the particle model enable us to explore nonequilibrium dynamics of volcano, as well as

*E-mail address: yukawa@ap.t.u-tokyo.ac.jp

†E-mail address: ito@ap.t.u-tokyo.ac.jp

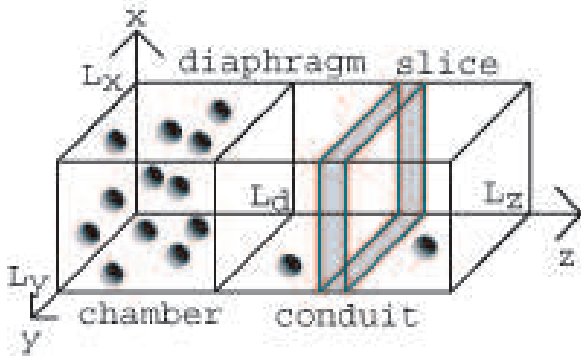


Fig. 1. Geometry of the system. When we calculate physical quantities, we slice the system with a unit length.

the model can verify an macroscopic theoretical model.

Here we assume microscopic dynamics are governed by the following Hamiltonian:

$$\mathcal{H} = \sum_{i=1}^N \frac{\mathbf{p}_i^2}{2m_i} + \frac{1}{2} \sum_{i,j} \alpha_i \alpha_j \phi(|\mathbf{q}_i - \mathbf{q}_j|), \quad (1)$$

where $\phi(r)$ is Lennard-Jones 12-6 potential: $\phi(r) = 4\epsilon\{(\sigma/r)^{12} - (\sigma/r)^6\} + \phi_0$. For computational efficiency, we introduce a potential cutoff as 3.9σ and determine the value of ϕ_0 to be $\phi(3.9\sigma) = 0$. And N denotes total particle number, m_i denotes mass of particle i , \mathbf{p}_i and \mathbf{q}_i denote particle three-dimensional momenta and coordinates, respectively. Dimensionless parameters α_i and $m_{\text{gas}}/m_{\text{magma}}$ are selected so that it will reproduce similar properties as magma gas;⁴ We take α_i to be 1 for magma particles, and 0.1 for gas particles. It determines energy scales of magma and gas. Ratio of melting temperatures of magma to gas is given by $\alpha_{\text{magma}}^2/\alpha_{\text{gas}}^2$ and it is 100 in the present model, although it is approximately 1000 for actual magma and gas. Present choice is ten times less than actual situation, but it is sufficient to describe the explosive eruption as we will show in the following. Particle mass ratio is chosen as $m_{\text{gas}}/m_{\text{magma}} = 0.1$, which is of order actual mass ratio. Hereafter we measure length, mass, and energy by the units of σ , m_{magma} and ϵ , respectively, and use dimensionless variables. Employing the Lennard-Jones 12-6 potential makes us to describe thermodynamic phases of gas, fluid, solid, and their coexisting state.

Using the above Hamiltonian, we calculate particle motion. The geometry of the system is as follows (see also Fig. 1): Consider rectangular parallelepiped with a size $L_x \times L_y \times L_z$. For x and y directions, periodic boundary conditions are imposed. A eruption direction is to z axis, and we prepare elastic walls at bottom and top. These walls are represented by repulsion part of Lennard-Jones potential.

First we have to prepare initial state as thermal equilibrium one. In this stage, whole system is divided into two parts, ‘‘chamber’’ ($0 \leq z \leq L_d$) and ‘‘conduit’’ ($L_d \leq z \leq L_z$) by a diaphragm, which is located at $z = L_d$, made of same elastic walls at $z = 0$ and $z = L_z$. At the beginning, magma and gas particles are contained in the chamber. Contrarily, only gas particles are in the

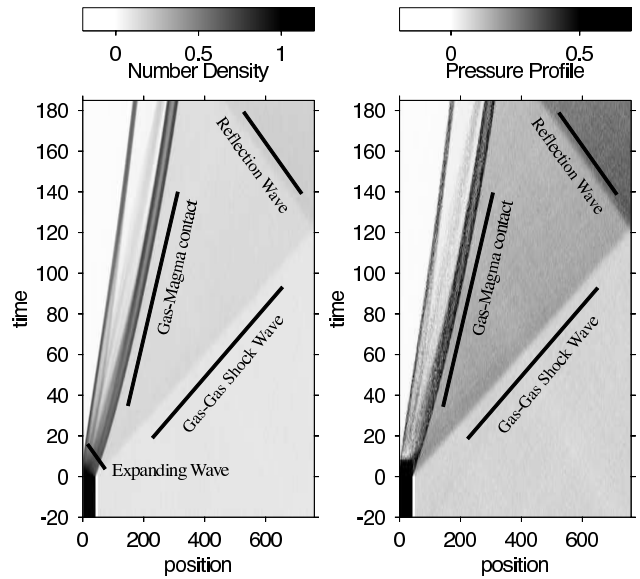


Fig. 2. Space-time profile of number density (left) and local pressure (right): Horizontal axis represents coordinate of explosion direction (z axis) and vertical axis is time. At time 0, a diaphragm is removed. Characteristic waves are guided by lines.

conduit. For preparing initial state, we do an isothermal simulation with Noé-Hoover thermostat in each part of the system.^{14–16} Density and temperature in the chamber are chosen as gas particles are uniformly mixed into magma particles; There is no phase separation.

After thermalization, we remove the separator between conduit and chamber and we detach the thermostat. Then the system obeys the Hamiltonian dynamics. If pressure in the chamber is higher than one in the conduit, an explosion is activated.

Simulation details are as follows: The second order symplectic method (the leapfrog method) is used in numerical integration. Time integration slice is taken to be 10^{-3} . This value is sufficient for present simulations, which is checked by energy conservation.

In the simulation, we calculate several physical quantities in boxes which are obtained by slicing along z -direction with a unit length σ .^{17,18} Number density $n(z)$ and mass density $\rho(z)$ of the slice z are basic quantities of macroscopic dynamics defined by counting a number and mass in the local slice. Barycentric velocity $\mathbf{v}(z)$ is defined through sum of momenta in the slice. Pressure $p(z)$, is defined by a trace of stress tensor. And temperature $T(z)$ is defined by variance of particle velocities from local barycentric motion.

Here we present a typical result of simulation as space-time profile of physical quantities. In Figs. 2, number density $n(z)$ and pressure $p(z)$ are presented. In this simulation, we take following parameters: System size is $L_x = L_y = 40$, $L_z = 740$. In an initial thermal equilibration stage, a diaphragm is located at $z = 40$, so the size of magma chamber is $40 \times 40 \times 40$ and one of the conduit is $40 \times 40 \times 700$. Total number of particle is 176 000, which consists of 57 600 magma particles and 118 400 gas particles. The chamber contains 57 600 magma particles and 6 400 gas particles. Other 112 000 gas particles are

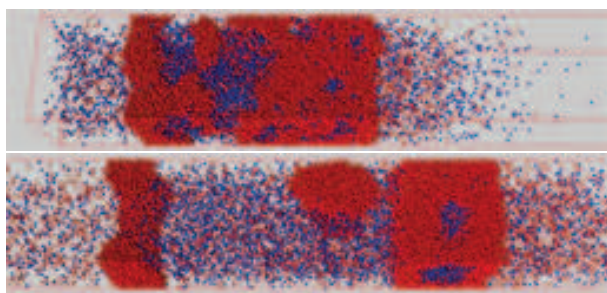


Fig. 3. (Color online) Snapshots of simulation: (Up) Snapshot at $t = 40$. (Down) Snapshot at $t = 170$. Parameters are identical to ones of Fig. 2. Eruption propagates to the right direction. Only particles originated from the chamber are plotted; A red ball represents a magma particle, and blue one is a gas particle. At the initial condition $t = 0$, blue and red particles are uniformly mixed in the chamber.

in the conduit. Then initial number densities are 1 for the chamber and 0.1 for the conduit. Thermalization is done with the chamber temperature 2 and the conduit temperature 0.8.

In Figs. 2, a horizontal axis corresponds to z direction and explosion goes to right. A vertical axis represents time. At the time 0, the diaphragm is removed. In the profile of number density, we recognize two characteristic density waves. First one begins at $(z = 40, t = 0)$ and propagates to $(750, 120)$. This wave corresponds to a shock wave between hot gas, which is heated by adiabatic compressing, and thermal equilibrium gas. Its velocity is larger than a sound velocity of equilibrium conduit gas. This wave is reflected at $(757, 120)$, because an elastic wall exists at there. Another wave propagates more slowly than the shock wave from $(40, 0)$ to $(300, 185)$. Front position of this density wave corresponds to magma-gas contact surface.

There are other small waves in this figure. A wave propagating from $(0, 10)$ to $(170, 185)$ is also reflecting wave caused by the elastic wall located at $z = 0$. A wave propagating to opposite direction, which is from $(40, 0)$ to $(0, 10)$, is also observed in the figure. This wave is an expansion wave of dense magma-gas mixture.

Other significant features are observed in this space-time profile. After propagating magma-gas contact wave, some internal structures are glowing. To investigate the internal structure in details, we show snapshot of simulation are shown in Figs. 3. These snapshot are taken from the simulation drawing Fig. 2, so simulation parameters are identical ones of that simulation. We only draw magma particles and gas particles which are in the magma chamber at the initial condition. Gas particles coming from the conduit are omitted. Explosion propagates to the right direction in this figure, which is z axis.

Before removing the diaphragm, magma and gas are uniformly mixed in the magma chamber. But, in Figs. 3, inhomogeneous mixing of those components is gradually growing during the eruption. This reminds us of spinodal decomposition. Size of exsolved gas bubble grows from Figs. 3(a) to (b); In Fig. 3(a), bubble size are widely distributed but, in (b), one large gas bubble and small bubbles in the thick magma exists. In large gas bubble,

one magma droplet is observed.

In this way, magma-gas mixture become inhomogeneous mixture and internal structure of bubbles are growing. Such behavior is consistent with the scenario of volcanology. But in the present simulation, transition to magma dispersion flow is not observed. The reason may be that smaller cross section of conduit and finiteness particles.

Next we compare the present simulation results with the continuum description given by Woods.⁵ In his model, magma-gas mixture is described by one-dimensional nonviscotic compressible one-component fluid. The dynamics are described by a continuity equation, an equation of motion, and the followings:

$$\frac{1-n}{\rho_l} + \frac{nRT}{p_g} = \frac{1}{\rho}, \quad p_g \left(\frac{\phi}{\rho} \right)^{\gamma_m} = \text{const.}, \quad (2)$$

where $\rho, \rho_l, p_g, T, R, n, \phi$ and γ_m denote mass density, mass density of magma component, pressure of gas component, temperature, a gas constant, a mass fraction of magma and gas components, a volume fraction of magma and gas components, and ratio of specific heats, respectively. In these quantities, ρ, p_g, T and $\phi^{-1} \equiv 1 + \frac{1-n}{n} \frac{p_g}{\rho_l RT}$ are variables. Other ρ_l, R, n , and γ_m are fixed to some constant values. The first equation is an equation of states, and the second one expresses an isentropic condition derived from the first law of thermodynamics. As we know the present equation of states is almost identical to one of ideal gas.

These equations are essentially same as ones of compressible ideal gas fluid. To study the equations is just an textbook example.^{19,20} We get a standard rewrite as

$$\left\{ \frac{\partial}{\partial t} + (w \pm a(\rho)) \frac{\partial}{\partial z} \right\} \left(w \pm \int^{\rho} \frac{a(\rho')}{\rho'} d\rho' \right) = 0, \quad (3)$$

where w and $a(\rho)$ are a velocity field and a sound velocity, respectively. The sound velocity of magma-gas mixture is a function of ρ , and it is expressed as $a^2(\rho) = a_0^2(\rho/\rho_0)^{\gamma_m-1}(\phi_0/\phi)^{\gamma_m+1}$ (a_0, ρ_0, ϕ_0 are sound velocity, density, and volume fraction at some reference state.) This equation gives characteristic curves and conserved quantities on them. Then we can solve the equation in characteristic regions. For obtaining global shock tube solution, we have to glue the solution with appropriate boundary conditions.

In Fig. 4, temperature $T(z)$, barycentric velocity $\mathbf{v}(z)_z$, pressure $p(z)$, mass density $\rho(z)$ of the present simulation are shown. Simulation parameters are taken to be as follows: System size is $L_x = L_y = 32, L_z = 408$ and size of magma chamber is $32 \times 32 \times 200$. Initial number density of magma chamber is taken to be 1 and conduit density is 0.02, thus the number of particles in the chamber is 204 800, which contains 10% gas particles. The number of gas particles in the conduit is 4 096. In this simulation, we imposed an artificial boundary condition at the top of conduit; For decreasing reflection effects from the top elastic wall, we attach a particle sink at the top, in which particles with the energy larger than some threshold value are removed from the system.

We can observe characteristic regions in Fig. 4. Let us compare these results with continuum descriptions. The

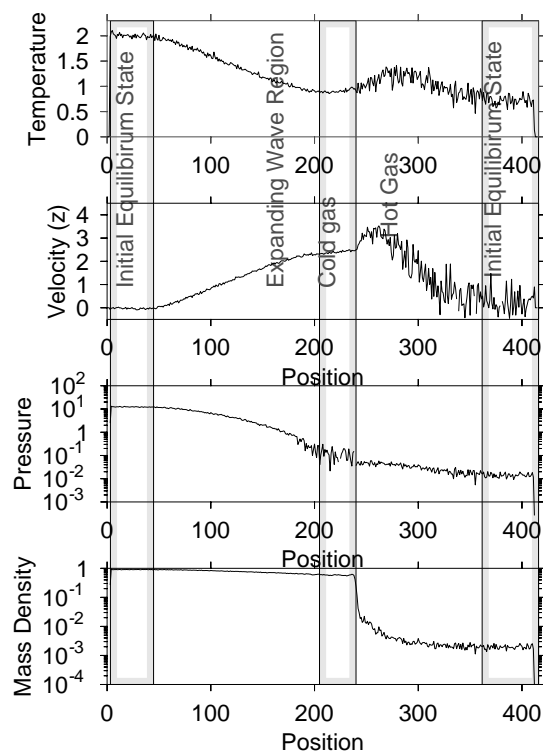


Fig. 4. Spatial profiles of temperature, velocity (z), pressure, and mass density at $t = 15$: System size is taken to be $L_x = 32$, $L_y = 32$, $L_z = 408$ and size of magma chamber is $32 \times 32 \times 200$. Initial mass density and temperature are taken to be 1 and 2, respectively. We can recognize characteristic regions. From right, “initial equilibrium state”, “hot gas region”, “cold gas region”, “expanding wave region”, and “initial equilibrium state” again are observed. These regions are indicated by gray rectangular.

solution of Eq. (3) teaches us that there are three regions in shock tube analysis, that is, a hot gas region, a cold gas region, and an expanding wave region. Corresponding regions of simulation are indicated in the figure; In the “hot gas” region, gases are heating up by the shock wave. In contrast, in the “cold gas” region, gases are cooling by an adiabatic expansion. Another region is an “expanding wave” region in which the expanding wave exists and physical quantities are smoothly changed. Physical properties of such regions obtained by the simulation are almost equivalent to ones of shock tube analysis. But there is a little mismatch with the solution; Analysis of compressible fluid gives constant profiles of physical quantities in both hot and cold gas regions. But, in this simulation, some structures are observed in each regions. For example, in a velocity profile of the hot gas region, velocity near cold gas is rather faster than other areas. This high velocity area is caused by pushing effects of magma-gas contact surface, which is corresponding to the front of cold gas contact. These high velocity particles are not thermalized yet; In the molecular dynamics simulation, microscopic relaxation is apparently observed.

To summarize, we have constructed a microscopic model of Vulcanian eruption by a two-components Lennard-Jones particle system. We observed that the particle dynamics is efficient in this kind of dynamics. Using the present model we can reproduce characteris-

tic features of explosive eruption such as a shock wave, a expansion wave. At the early stage of the eruption, we also compare the simulation result with the analytic model given by Woods. Qualitative behavior is almost consistent with the analytic result, even though the flow is treated as nonviscotic one in the analytic model. In addition, we have also observed that the internal structure is growing during the eruption. Internal bubble structure cannot be captured by the Woods model. This behavior is also consistent with a eruption picture of volcanology study. Thus we conclude that the present model is a candidate of “an Ising model of Vulcanian eruption”.

To establish the present model, a quantitative study is inevitable. For this purpose, we have to enlarge the size of system; A transition from bubbly magma flow to magma dispersion flow will be reproduced and studied by simulation of the system with ten times larger to all directions. And the more details of volcanic eruption not only Vulcanian but also Strombolian, and Plinian will be elucidated. Present typical computational time is approximately 80 hours for 208 896 particles with single AMD opteron 248 (2.2GHz). Hence much larger simulation is feasible with large super computers.

Acknowledgments

The authors thank T. Koyaguchi for valuable discussion and comments. This work is partially supported by the Ministry of Education, Science, Sports and Culture, Grant-in-Aid for Scientific Research Priority Areas, No.14080204, 2005. The part of computation in this work has been done using the facilities of the Supercomputer Center, Institute for Solid State Physics, University of Tokyo and the Earth Simulator Center, Japan Agency for Marine-Earth Science and Technology.

- 1) O. Melnik and R. S. J. Sparks: *Nature* **402** (1999) 37.
- 2) O. Melnik: *Bull. Volcanol.* **62** (2000) 153.
- 3) T. Koyaguchi: *J. Volcanol. Geotherm. Res.* **143** (2005) 29.
- 4) H.-U. Schmincke: *Volcanism* (Springer-Verlag, Berlin, 2004).
- 5) A. W. Woods: *Nucl. Eng. Design*, **155** (1995) 345.
- 6) Y. Zhang, B. Sturtevant, and E. M. Stolper: *J. Geophys. Res.* **102** (1997) 3077.
- 7) B. Cagnoli, A. Barmin, O. Melnik, R. S. J. Sparks: *Earth Planet. Sci. Lett.* **204** (2002) 101.
- 8) O. Spieler, D. B. Dingwell, and M. Alidibirov: *J. Volcanol. Geotherm. Res.* **129** (2004) 109.
- 9) M. Ichihara, D. Rittel, and B. Sturtevant: *J. Geophys. Res.* **107**(B10), 2229, doi:10.1029/2001JB000591, (2002).
- 10) T. Ishiwata, T. Murakami, S. Yukawa, and N. Ito: *Int. J. Mod. Phys.* **C15** (2004).
- 11) T. Murakami, T. Shimada, S. Yukawa, and N. Ito: *J. Phys. Soc. Jpn.* **72** (2003) 1049.
- 12) H. Okumura and N. Ito: *Phys. Rev.* **E67** (2003) 045301(R).
- 13) H. Okumura and D. M. Heyes: *Phys. Rev.* **E70** (2004) 061206.
- 14) S. Nosé: *Mol. Phys.* **52** (1984) 255.
- 15) S. Nosé: *J. Chem. Phys.* **81** (1984) 511.
- 16) W. G. Hoover: *Phys. Rev.* **A31** (1985) 1695.
- 17) J. H. Irving and J. G. Kirkwood: *J. Chem. Phys.* **18** (1950) 817.
- 18) J.-P. Hansen and I. R. McDonald: *Theory of Simple Liquids* (Academic Press, Amsterdam, 1986).
- 19) H. Lamb: *Hydrodynamics* (Dover, New York, 1945).
- 20) L. D. Landau and E. M. Lifshitz: *Fluid Mechanics* (Pergamon Press, Oxford, 1959).